Bull. Mater. Sci., Vol. 29, No. 5, October 2006, pp. 485–490. © Indian Academy of Sciences.

Morphology, crystallization and dynamic mechanical properties of PA66/nano-SiO_2 composites

HUIMIN LU, XIANGMIN XU, XIAOHONG LI and ZHIJUN ZHANG*
Key Lab for Special Function Material, Henan University, Kaifeng 475001, China

MS received 20 March 2006; revised 1 July 2006

Abstract. This article addresses the effect of nano-SiO_2 on the morphology, crystallization and dynamic mechanical properties of polyamide 66. The influence of nano-SiO_2 on the tensile fracture morphology of the nanocomposites was studied by scanning electron microscopy (SEM), which suggested that the nanocomposites revealed an extensive plastic stretch of the matrix polymer. The crystallization behaviour of polyamide 66 and its nanocomposites were studied by differential scanning calorimetry (DSC). DSC nonisothermal curves showed an increase in the crystallization temperature along with increasing degree of crystallinity. Dynamic mechanical properties (DMA) indicated significant improvement in the storage modulus and loss modulus compared with neat polyamide 66. The tan ä peak signifying the glass-transition temperature of nanocomposites shifted to higher temperature.

Keywords. Polyamide 66; nano-SiO_2; morphology; crystallization; dynamic mechanical properties.

1. Introduction

Recently, according to the development of the nanotechnique, there has been a growing interest in the field of polymer based nanocomposites due to their special properties (Tjong *et al* 2002; Wu 2002; Liu *et al* 2005), not only can they provide properties of traditional composites, but also exhibit unique optical, electric, and magnetic properties. Compared to other traditional materials, nanocomposite has attracted considerable interest both in industry and academia because of its significantly improved thermal properties, solvent resistance, gas permeability and mechanical property.

Nano-SiO_2 is the most commonly used tool for the preparation of nanocomposites. Nano-SiO_2 particles are hydrophilic because of surface OH groups and so need to be modified with organic surfactant treatment. So the treatment of the particle is the key issue in the process. In this paper, we introduce a new route of synthesizing superhydrophobic nanoscale silica by surface-modification *in situ* in aqueous solution (Li *et al* 2006). We present the typical formula and technique used in our study, below.

Polyamides are considered to be one of the most important super-engineering materials because of their superior mechanical properties at elevated temperature due to their thermal stability. Polyamide based nanocomposites was first reported by Fujiwara and Sakamoto (1976). Recently, there have been many studies concerning polyamide based nanocomposites on the morphology (Fornes and Paul 2003), crystallization and dynamic mechanical properties (Xie *et al* 2005a). Adding montmorillonite to nylon6 increases the tensile modulus, yield strength, heat-distortion temperature (Kojima *et al* 1993a,b; Xie *et al* 2005b) and also improves the barrier (Kojima *et al* 1993c) and ablative (Vaia *et al* 1999) properties. The nano-dispersed silicate platelets can induce cavitations and fibrillation of the matrix polymer during tensile of fatigue experiments (Gloaguen and Paul 2001; Bellemare *et al* 2004). It has also been reported that 1 wt% of poly(*n*-butyl acrylate) (PBA) encapsulated MWNT melt mixed with PA6 enhanced the interfacial adhesion between PA6 and MWNT (Xia *et al* 2003). The crystallization behaviour of PA mixed with nano filler has been reported by many workers. The isothermal crystallization behaviour of PA6/MMT nanocomposites have been studied by Fornes and Paul (2003). The effect of silicate platelets on the crystal structure of nylon 6 matrix of nanocomposites have also been of interest. Early investigations by Liu *et al* (1999) suggest that the *g*-crystalline form is enhanced by the addition of clay, which is significant since crystalline structure may affect physical and mechanical properties. This leads to increased yield strength and tensile modulus of composites compared to pure PA6. In this article, we report the preparation of PA66/nano-SiO_2 composites by a melt blending technique. As we know, although there are many reports on the preparation of PA66 based nanocomposites, this is the first report involving nano-SiO_2 particles. The morphology, crystalline and dynamic mechanical properties of PA66 and its nanocomposites were studied.

*Author for correspondence (luhuim@126.com)

2. Experimental

2.1 *Materials and preparation of nanocomposites*

The PA66 pellets (EPR27) were provided by China Shenma Group Nylon 66 Salt Co. Ltd. SiO_2 nanoparticles (preparated in-house) were surface modified *in situ*. Nanocomposites with different contents of SiO_2 nanoparticles were prepared by melt-compounding using a twin extruder with temperatures of zone I–V being 270°C, 275°C, 275°C, 270°C, 275°C, respectively, and head temperature at 280°C. For comparison, neat PA66 was also extruded in the twin extruder at the same processing conditions. Followed by pelletizing, the materials were vacuum dried and injected to standard testing specimens for characterization and tests. The codes and composites are summarized in table 1.

2.2 *Measurement and techniques*

2.2a *Scanning electron microscopy*: To observe the tensile fractured surfaces of neat PA66 and its nanocomposites, the fracture surfaces were coated with thin layers of gold of about 100 A. All specimens were examined with JSM5600LV scanning electron microscope.

2.2b *Differential scanning calorimetry*: The crystallization behaviour of PA66 and its nanocomposites was determined using a Q-100 thermal analysis apparatus. The heating–cooling–heating cycles were recorded in the temperature range 0 ~ 290°C at a scan rate of 10°C/min under nitrogen atmosphere. In the first heat run, all samples were annealed at 290°C for 5 min to eliminate the thermal history. The degree of crystallinity (X_c) of PA66 and its nanocomposites was calculated from the heat of fusion (ΔH_m) of the second heating cycle with the following relation:

$$X_c = \{\Delta H_m/(1 - \Phi)\Delta H_m^0)\} \times 100\%, \quad (1)$$

where ΔH_m^0 is the heat of fusion for 100% crystalline PA66, which was taken as 196 $J \cdot g^{-1}$ (Brandrup and Immergut 1989) and Φ the weight fraction of the filler in the composites.

2.2c *Dynamic mechanical analysis*: The dynamic mechanical tests were carried out on a dynamic mechanical thermal analysis (Q-800, TA C. UK) with the temperature range from –50 ~ 200°C. The frequency used was 1 Hz and the heating rate, 5°C/min. The specimen dimension was $24 \times 6 \times 1{\cdot}5$ mm^3.

Table 1. Codes and composites.

Sample code	Compositions (wt%)
PA66	PA66 (100)
PNSC-1	PA66 (99) + nano-silica (1)
PNSC-3	PA66 (97) + nano-silica (3)

3. Results and discussion

3.1 *Preparation and characterization of dispersible nano-SiO_2*

The reagents such as sodium metasilicate and hydrochloric acid were analytical pure reagents (AR). Hexamethyldisilazane (HMDS) was purchased from Nanjing Crompton Shuguang Organosilicon Co., China. They were used without further treatment.

Sodium metasilicate was dissolved into deionized water at a certain concentration in a reactor equipped with a condensator and two dropping funnels of constant pressure. The weighed HMDS dissolved in absolute alcohol as the modifier was placed into the other funnel. Solution of hydrochloric acid and deionized water was poured into one dropping funnel. A certain quantity of modifier dissolved in absolute alcohol was placed into the other funnel. At first, we added half of hydrochloric acid solution to the reactor under stirring. Then the residual hydrochloric acid and modifier were added dropwise into the reactor simultaneously. When the concentration of sodium metasilicate was equal to that of hydrochloric acid, the reaction solution appeared turbid. Gradually, an amount of foam appeared on the surface of this aqueous solution. The suspension was heated to 60°C and was stirred for 4 h at this temperature. Then the obtained solution was put into a separating funnel. The suspension was separated into two layers quickly, and a layer of white floc floated on the top. The clear aqueous solution at the bottom was dropped out thereafter. The floc was collected by filtration and washed repeatedly using a mixed solution of deionized water and alcohol until Cl^- could not be detected using silver nitrate solution by visual examination. Here, Cl^- and Nat were removed at the same time. The filtered cake was redispersed into a quantity of mixed solution of deionized water and alcohol at a volume ratio of 1 : 1 to form emulsion. Finally, the emulsion was spray-dried and loose SiO_2 nanoparticles were obtained (with a yield rate of over 93% measured based on Si of sodium metasilicate and HMDS). Surface-modification of such nanosilica *in situ* is a polyreaction-like process where the hydrolysis product of sodium metasilicate is used as the monomer and HMDS as the chain terminator. The condensation polymerization of hydrolysis products is a process of chain growth and surface-modification is analogous to chain termination. We hypothesize that the condensation-like polymerization is carried out in the following mode:

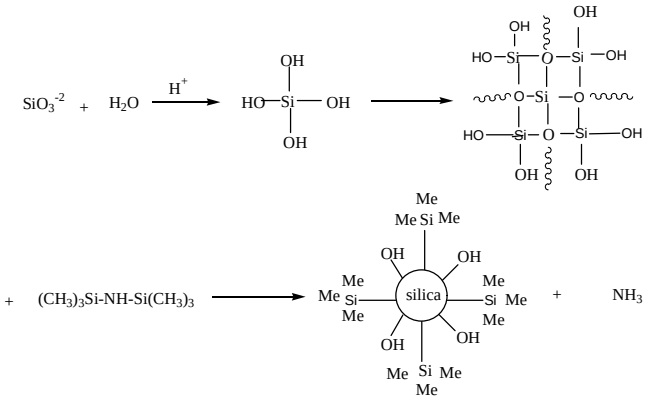

where Me stands for $–CH_3$. The bulky $–CH_3$ that is conjoint to Si makes the methyl groups to repulse each other and displace, which leads to have superior dispersivity and stability in many types of organic solvents and polymer, however, the –OH can combine with PA66 by hydrogen bonding.

Transmission electron microscopic (TEM) analysis was performed with a JEM-2010 microscope. Infrared spectrum was obtained using a Nicolet 170sx Fourier transform infrared spectrophotometer.

From the FTIR spectrum of DNS in figure 1, the bands near 1380 cm^{-1} correspond to the asymmetric stretching vibration peak of C–H. The peak of 938 cm^{-1} corresponds to the absorption band of Si–O–C. TEM photographs of the typical DNS dispersed in absolute alcohol are given in figure 2. The morphology of DNS is well distributed with size, 15–20 nm.

3.2 *Mechanical properties*

The mechanical properties of PA66/SiO_2 nanocomposites are summarized in table 2. It can be seen that the tensile strength of PA66 increased by 7% with the addition of 3 wt% nano-silica. It is also noted that the tensile modulus increases significantly upon formation of the nanocomposites. This beneficial effect is believed to arise from an improvement in the compatibility between the nano-silica and PA66 matrix which increases the stiffness at the expense of toughness of the composites. Nanocomposites exhibit an increase in the elongation at break with increasing nano-silica concentration. This observation may be explained in terms of more efficient load transfer with higher nano-silica concentration, which facilitates plastic deformation.

3.3 *Tensile fracture morphologies of neat PA66 and its nanocomposites*

The tensile fracture morphologies of neat PA66 and its nanocomposites were investigated by means of SEM. Figure 3 presents micrographs of the overall (a3, b1, c1) (at a lower magnification) and partial (a2, b2, c2) (at a higher magnification) fractured surfaces. The neat PA66 material shows a relatively smooth fracture surface, which is a typical brittle rupture (a1 and a2). The nanocomposites reveal a coarser fracture pattern at low magnification (b1 and c1). From figure 3 (b2 and c2), the nanocomposites reveal an extensive plastic stretch of the matrix polymer. The mild profiles of the deformation circles (as indicated by the arrows in figure 3, c2) suggest a low plastic deformation level.

As shown in figure 1, it can be seen that the addition of nano-silica can have an obvious effect on the fracture behaviour of PA66. The addition of DNS nano-silica greatly increased not only the tensile strength and modulus but also the toughness, which may be caused by the enhanced interfacial interaction between nylon 66 and nano-silica.

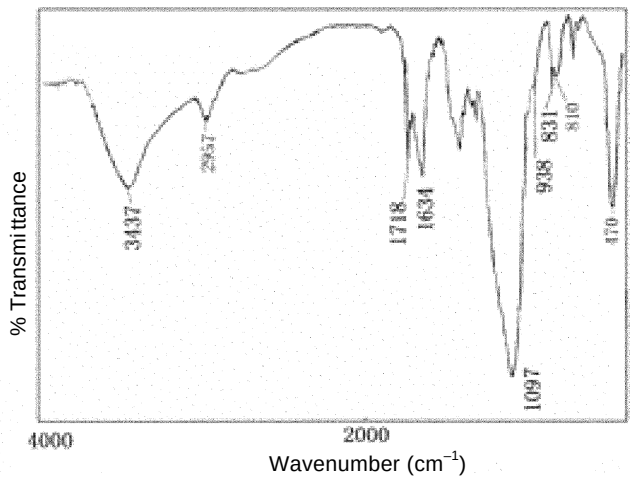

Figure 1. FT–IR spectra of SiO_2 nanoparticles.

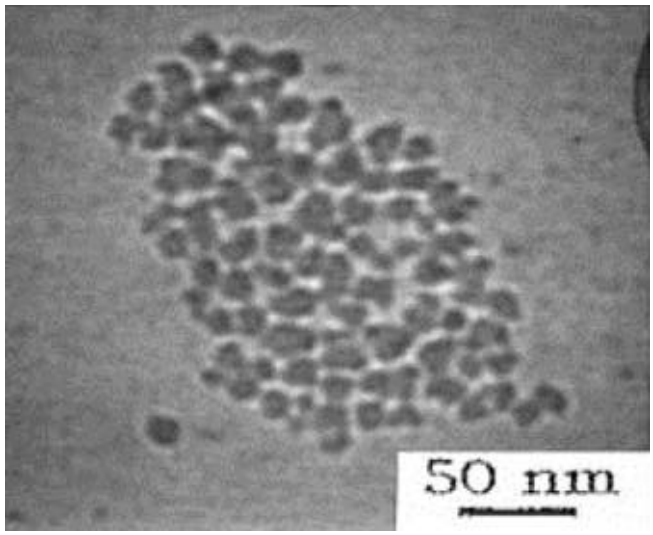

Figure 2. TEM image of SiO_2 nanoparticles.

Table 2. Mechanical properties of PA 66/SiO_2 nanocomposites.

Sample	Tensile strength (MPa)	Tensile modulus (MPa)	Elongation at break (%)
PA66	50·7	1708	19
PNSC-1	53·0	2383	30
PNSC-1	54·2	2385	32·7

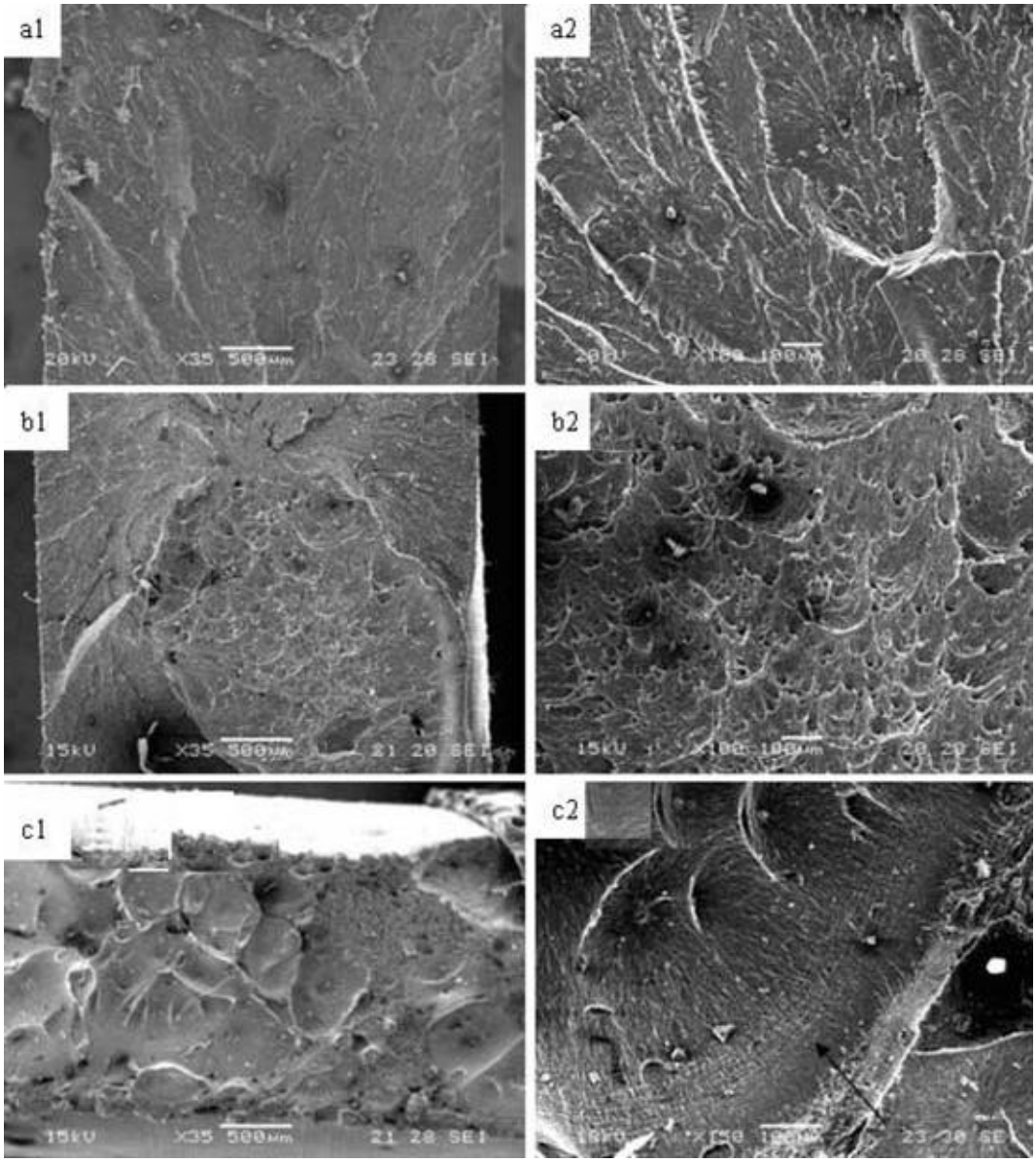

Figure 3. The tensile fracture of PA 66 and its nanocomposites.

3.4 *Crystallization properties*

Nonisothermal crystallization of PA66 and its nanocomposites was studied and DSC curves are presented in figure 4. Figure 4a shows the cooling scans and figure 4b the heating scans. Heating scans were analysed for the melting temperature, T_m, heat of fusion, ΔH_m, and the degree of crystallinity, X_c, while cooling scans were used to obtain the crystallization temperature, T_c, and the degree of super cooling, $\Delta T = (T_m - T_c)$. The heat of fusion was determined by integrating the heat flow at 240–270°C.

The result clearly indicated that nano-SiO_2 in PA66 could improve the crystallization of polymer matrix, since the crystallization temperature increased by 3°C. The degree of crystallinity of PA66 in PA66/nano-silica composites also increased especially at the higher nano-

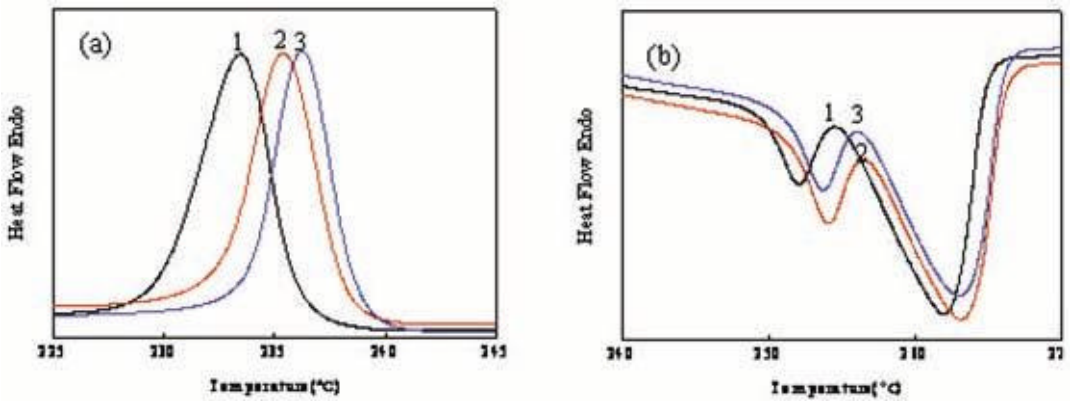

Figure 4. (**a**) DSC crystallization exotherms of PA66 and its nanocomposites and (**b**) DSC melting endotherms during the second heating cycle of PA 66 and its nanocomposites.

Table 3. DSC melting and crystallization parameters for PA66, PNSC-1 and PNSC-3.

Sample	T_m (°C)	T_c (°C)	ΔT (°C)	ΔH_m (J·g^{-1})	X_c (%)
PA66	262·0	233·5	28·5	57·98	29·6
PNSC-1	262·14	235·8	26·34	62·96	32·1
PNSC-3	262·07	236·7	25·37	66·13	33·7

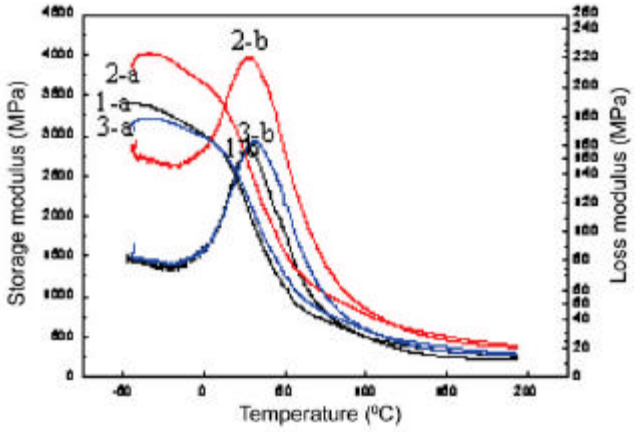

Figure 5. Plots of storage modulus and loss modulus versus temperature of nylon 66 and nanocomposites.

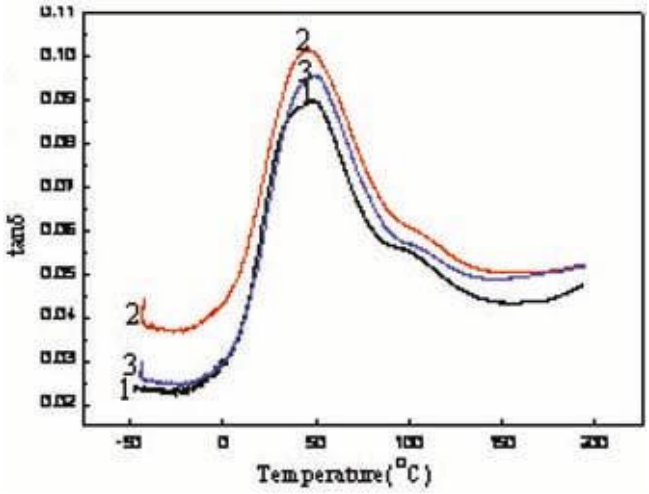

Figure 6. Plots of tan *d* vs temperature of nylon 66 and nanocomposites.

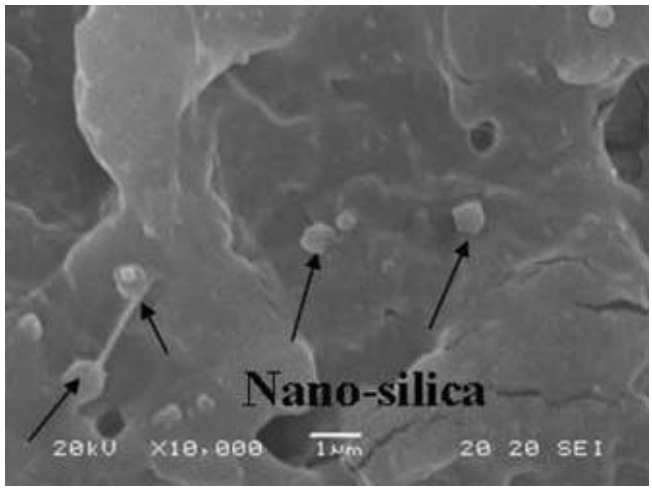

Figure 7. The tensile fracture at a higher magnification of PNSC-3.

silica content (the degree of crystallinity increased by 17·8%). Table 3 also shows that the ΔT of nanocomposites are smaller than that of neat PA66, which indicates that the addition of nano-silica into PA66 increased the rate of crystallization of PA66 (Wu *et al* 2002).

It can also be seen from table 3 that the melting temperature (T_m) remained unaltered after the addition of nano-silica, which means that the crystal size of PA66 did not change. Interestingly, we found a double melting endothermic peak in the second heating run (figure 4b), indi-

cating the existence of either mixed crystal structure of PA66 or a process related to melting-recrystallization during heating. A similar observation was reported for PA66/SWNT composites by Bhattacharyya *et al* (2005).

3.5 *Dynamic mechanical properties*

DMA is often used to study relaxations in polymers. An analysis of storage modulus, loss modulus, and tan δ is very useful in ascertaining the performance of a sample under temperature.

The storage modulus and loss modulus of PA66 and its nanocomposites depended on the temperature (as shown in figure 5). It was apparent that the storage modulus and loss modulus of PNSC-1 were higher than those of the neat PA66 throughout the whole temperature range, particularly from –50 ~ 20°C, the storage modulus and loss modulus of PNSC-1 improved by 17·7% and 109% at –40°C compared to neat PA66, respectively, which was due to the dispersion of surface-treatment SiO_2 nanoparticles in the matrix and increased interfacial area. As a result, interaction between the filler and the matrix was strengthened and the blending effect of SiO_2 surface on the motion of the matrix molecular chain, as well as the friction between them increased. But the storage modulus and loss modulus of PNSC-3 decreased which was due to the aggregation of SiO_2 nanoparticles in the matrix (as shown in figure 7). However, from 36 ~ 200°C, the storage modulus and loss modulus of PNSC-3 are higher than those of neat PA66.

From figure 6 we can see that the T_g of PA66 determined from the maxima of tan δ in DMA investigation of PA66 increased from 47–53°C after the addition of 3 wt% nano-SiO_2. Since the glass transition process is related to the molecular motion, the T_g is considered to be affected by molecular peaking, chain rigidity and linearity (Li *et al* 1999). The increase in the T_gs of PNSC-1 and PNSC-3 in comparison with the neat PA66 can be attributed to maximizing the adhesion between polymer and organically modified nano-SiO_2 particles because of the nanometer size which restricts segmental motion near the organic–inorganic interface which is a typical effect for the inclusion of nano-SiO_2 in a polymer system (Al-Kandary *et al* 2005).

4. Conclusions

(I) A novel method of preparation of superhydrophobic nanosilica by surface-modification *in situ* in aqueous solution is reported in this paper.

(II) We have shown that PA66/nano-SiO_2 composites can be prepared by a melt compounding technique with organically modified nano-SiO_2.

(III) The SEM results of the nanocomposites showed an extensive plastic stretch of the matrix polymer. The nonisothermal crystallization studies showed an enhanced crystallization of PA66.

(IV) DMA indicated 109% improvement in loss modulus for 1 wt% PA66/nano-SiO_2 composites compared to neat PA66 at –40°C.

(V) The increase in glass-transition temperature in PNSC-3 by ~ 6°C is attributed to restricted chain mobility in the nanocomposites.

References

Al-Kandary Sh, Ali A M and Ahmad Z 2005 *J. Appl. Polym. Sci.* **98** 2521

Bellemare S C, Bureau M N, Denault J and Dickson J I 2004 *Polym. Compos.* **25** 433

Bhattacharyya A R, Pötschke P, Häuâler L and Fischer D 2005 *Macrochem. Phys.* **206** 2084

Brandrup J and Immergut E H 1989 *Polymer handbook* (New York: J. Wiley Sons) 2nd ed.

Fornes T D and Paul D R 2003 *Polymer* **44** 3945

Fujiwara S and Sakamoto T 1976 Japanese Patent No. 109998

Gloaguen J M and Paul D R 2001 *Polymer* **42** 1083

Kojima Y, Usuki A, Kawasumi M, Okada A, Fukushima Y, Kurauchi T and Kamigatio O 1993a *J. Mater. Res.* **8** 1179

Kojima Y, Usuki A, Kawasumi M, Okada A, Fukushima Y, Kurauchi T and Kamigatio O 1993b *J. Polym. Sci. Polym. Chem. Ed.* **31** 983

Kojima Y, Usuki A, Kawasumi M, Okada A, Fukushima Y, Kurauchi T and Kamigatio O 1993c *J. Appl. Polym. Sci.* **49** 1259

Li F, Ge J and Honigfort P S 1999 *Polymer* **40** 4987

Li X H, Cao Z, Liu F and Zhang Z J 2006 *Chem. Lett.* **35** 94

Liu H Z, Zheng S X and Nie K M 2005 *Macromolecules* **38** 5088

Liu L, Qi Z and Zhu X 1999 *J. Appl. Polym. Sci.* **71** 1133

Tjong S C, Meng Y Z and Hay A S 2002 *Chem. Mater.* **14** 44

Vaia R A, Price G, Ruth P N, Nguyen H T and Lichtenhan J 1999 *J. Appl. Clay Sci.* **15** 67

Wu C L, Zhang M Q, Rong M Z and Friedrich K 2002 *Comp. Sci. Technol.* **62** 1327

Wu Z G, Zhou C X and Zhu N 2002 *Polym. Testing* **21** 479

Xia H, Wang Q and Qiu G 2003 *Chem. Mater.* **15** 3879

Xie S B, Zhang Sh M and Zhao B 2005a *Polym. Int.* **54** 1673

Xie S, Zhang S, Wang F, Liu H and Yang M 2005b *Polym. Eng. Sci.* **45** 1247